Biosensors and Bioelectronics 71 (2015) 214–221

Contents lists available at ScienceDirect

Biosensors and Bioelectronics

journal homepage: www.elsevier.com/locate/bios

Electrochemical detection of Bisphenol A with high sensitivity and selectivity using recombinant protein-immobilized graphene electrodes

Kwang Su Kim [a,1], Ji-ryang Jang [a,1], Woo-Seok Choe [a,b,*], Pil J. Yoo [a,b,*]

[a] SKKU Advanced Institute of Nanotechnology (SAINT), Sungkyunkwan University, Suwon 440-746, Republic of Korea
[b] School of Chemical Engineering, Sungkyunkwan University, Suwon 440-746, Republic of Korea

ARTICLE INFO

Article history:
Received 27 February 2015
Received in revised form
6 April 2015
Accepted 13 April 2015
Available online 14 April 2015

Keywords:
Electrochemical impedance spectroscopy
Bisphenol A
Reduced graphene oxide
Recombinant Lac repressor
Biosensor

ABSTRACT

A novel Bisphenol A (4,4'-isopropylidenediphenol, BPA) sensor was developed harnessing an electrochemical platform comprising a layer-by-layer assembled reduced graphene oxide (rGO) electrode and a designer probe specifically recognizing BPA. The BPA detection probe, a recombinant protein (LacI-BPA), was constructed by fusing a disulfide-constrained high affinity BPA binding peptide (CKSLENSYC) to the C-terminus of Lac repressor (LacI). Following expression and purification, the LacI-BPA was heat-denatured on-purpose to facilitate its direct adhesion on the rGO electrode surface via pi-stacking interaction. When the performance of the fabricated BPA sensor (LacI-BPA/rGO) was assessed by electrochemical impedance spectroscopy (EIS), it showed a wide linear dynamic range of BPA detection spanning from 100 fM to 10 nM. Moreover, our BPA sensor exhibited negligible cross reactivity to BPA analogs such as Bisphenol S (BPS) and Bisphenol F (BPF) and almost complete spike recovery of BPA from plastic extracts containing various potential interferents. With these merits, the BPA sensor developed in the present study is expected to find practical application in selective and sensitive detection of BPA from diverse sample solutions.

1. Introduction

Bisphenol A (BPA), formed by a condensation reaction between one acetone and two phenol molecules, is a major monomeric material for synthesizing polycarbonate plastics (CDs, automotive parts, baby water bottles, containers and lens of glasses) and epoxy resin (food cans, packing materials) (Vom Saala and Hughes, 2005). While it has been broadly used for household and industrial purposes, a concern on the toxicity of BPA as one of the endocrine disruptors has restricted its use for practical applications (Kuiper et al., 1998; Staples et al., 1998). A 2010 report from the United States Food and Drug Administration (FDA) stated its potential hazard particularly to infants and children. Since the BPA is easily leachable from household items, such as food packaging or plastic bottles, the public is highly vulnerable to BPA exposure and its toxicity (Vandenberg et al., 2007). Widespread daily exposure to low levels of BPA and the potential adverse effects arising from its hormone-like behavior causing diverse health concerns including cancers, diabetes and heart diseases have posed increasing threats to public health. Therefore, there is an urgent need to develop detection methods for monitoring BPA concentration with high sensitivity and selectivity.

At the early stage of developing BPA detection methods, analytical techniques included high-performance liquid chromatography (HPLC) (Kuroda et al., 2003; Lin et al., 2011), and gas chromatography (GC) (Altamirano et al., 2011). However, these methods are laborious, time-consuming and require multiple sample pre-treatment steps. Moreover, these instruments are rather expensive and cumbersome for easy and fast operation. Thus, there remains a need for developing a simple and low-cost detection method to determine the BPA level directly from samples with high reliability. To address this issue, alternative techniques exploiting optical (Rodriguez-Mozaz et al., 2005), fluorescent (Wang et al., 2006) and electrochemical (Kafi et al., 2011; Wang et al., 2014, 2012; Zhu et al., 2014) sensors have been pursued. In addition, other approaches such as optofluidics-based bioassay platform (Long et al., 2014), lateral flow strip (Mei et al., 2013a) and colorimeteric sensor (Mei et al., 2013b) have also been investigated for BPA detection. Among them, electrochemical

* Corresponding authors at: School of Chemical Engineering, Sungkyunkwan University, Suwon 440-746, Republic of Korea. Fax: +82 31 2907272.
E-mail addresses: checws@skku.edu (W.-S. Choe), pjyoo@skku.edu (P.J. Yoo).
[1] These authors contributed equally to this work.

http://dx.doi.org/10.1016/j.bios.2015.04.042
0956-5663/

impedance spectroscopy (EIS) has shown great potential because of the fast response, low cost, and good operability. Simply by measuring the response of an electrochemical system over a wide range of frequency, EIS provides highly sensitive impedimetric signals to the binding event of target species on the electrode surface (Macdonald, 1987).

To implement high performance EIS sensors, it is important to choose the relevant electrode with good electrical conductivity and electrochemical responsivity. For the recognition of important small molecules, there are various types of electrochemical sensors with unique platforms (Cao et al., 2014; Kubesa et al., 2014; Stobiecka et al., 2012; Stobiecka and Chałupa, 2015; Stobiecka and Hepel, 2011). Graphene related materials, such as chemical vapor deposited (CVD) graphene or reduced graphene oxide (rGO) films, are favored as one of the most promising resources due to the advantageous aspects of thin film thickness and fast charge transport (Castro Neto et al., 2009; Geim and Novoselov, 2007). In addition, by applying surface functionalization process, graphene electrodes are readily engineered to exhibit excellent biocompatibility without sacrificing its intrinsic physical stability (Wang et al., 2010). Therefore, graphene-based electrodes have been extensively studied as new electrochemical sensors. In our previous work, we came up with a high-performance impedance sensing system harnessing the denatured protein directly deposited via pi-stacking interaction on the layer-by-layer (LbL) assembled rGO film (Kim et al., 2013). Although bovine serum albumin (BSA) was tested as a demonstrative example, the suggested approach can offer the extended applicability to various proteins that specifically capture the target molecules. Meanwhile, in another study, we immobilized a cysteine-flanked heptapeptide sequence isolated through phage display technique on a gold electrode surface to form a self-assembled monolayer (Yang et al., 2014). This system showed high selectivity and practical applicability to BPA detection, but had a relatively low sensitivity with a limit of detection (LOD) around 1 nM. Therefore, it is expected to attain much enhanced sensitivity in BPA detection by introducing the rGO thin film electrodes.

The detection probe used in this study is a recombinant LacI protein (LacI-BPA) harboring a BPA-specific disulfide-constrained peptide moiety (CKSLENSYC) at the C-terminus (Yang et al., 2014). The rationale behind using the LacI protein as a docking platform is two-fold. First, LacI exhibits superb self-adhesion ability to the surfaces of various inorganic materials including novel metals (e.g. Au, Ag, Pt, Pd) and metal oxides (e.g. TiO_2, ZnO, WO_3, Cu_2O) often used as the electrodes for electrochemical sensor fabrication. Furthermore, the affinity of LacI towards these inorganic materials is retained regardless of whether the protein is in native or denatured form (unpublished data). Second, incorporation of a short-length peptide sequence to the C-terminus of the LacI does not compromise the intrinsic property of the protein (e.g. recognition of *lacO*) as demonstrated elsewhere (Chen et al., 2009), indicating that the C-terminal part is one of the permissive sites of LacI allowing the creation of engineered LacIs of varying properties. Besides, it was demonstrated that direct deposition of protein molecules on the extremely hydrophobic rGO electrode surface could be facilitated through pi-stacking interaction mediated by hydrophobic amino acid residues outwardly relocated on the protein surface upon denaturation (Kim et al., 2013). On the basis of these two-fold merits, LacI is therefore expected to provide a useful scaffold for designing a novel recombinant protein probe with high affinity to BPA (i.e. LacI-BPA). Moreover, the use of LacI-BPA in denatured form is reckoned to be conducive, without compromising its BPA recognition ability, to annealing of a BPA selective protein probe to the rGO electrode without tedious surface modification procedures often required to accommodate probe molecules lacking direct compatibility.

In this work, we developed a recombinant protein-based electrochemical sensor using rGO thin film electrode for highly sensitive and selective detection of BPA molecules. First, rGO thin film used as a working electrode was prepared using spin-assisted LbL assembly of GO nanosheets followed by thermal reduction to rGO. Then, the LacI-BPA probe was denatured by thermal treatment to enable its direct deposition on rGO surface through pi-stacking interaction. Structural and electrochemical changes on the rGO electrode arising from the LacI-BPA immobilization and the subsequent BPA capture were thoroughly characterized by atomic force microscopy (AFM), Raman spectra, and EIS analysis. Finally, when optimized for BPA detection, the presented EIS sensor showed remarkably high sensitivity capable of detecting BPA in the femtomolar range and good selectivity despite the presence of BPA analogs and/or other interferents in the mock samples.

The suggested strategy of using recombinant LacI as a protein probe for selective detection of a target analyte and direct coupling of the designer protein probe with varying electrode surfaces by harnessing intrinsic affinity and/or pi-stacking interaction is simple yet versatile. It is therefore expected to provide a generic tool for constructing efficient sensing platforms to detect various analytes with the use of target selective protein probes engineered and/or evolved from nature.

2. Experiment

2.1. Preparation of rGO thin film electrode

The details for synthesis of positively and negatively charged GO nanosheets were reported elsewhere (Park et al., 2011). Briefly, negatively charged GO was synthesized from graphite using a modified Hummers' method (Hummers and Offeman, 1958). To synthesize the positively charged GO, negatively charged GO was dried and went through acyl-chlorination reaction with excess amount of thionyl chloride, followed by amidation with ethylenediamine in pyridine solvent. To prepare the GO-assembled thin film electrodes of 2×2 cm^2, a quartz substrate was cleaned by sonication in ethanol and deionized (DI) water for 30 min each, and subjected to plasma treatment ($<$ 30 W, 0.1–0.5 Torr, PDC-001, Harrick Scientific Corp., NY) for 2 min to produce negatively charged surface. The spin-assisted LbL assembly using complimentarily charged GOs was carried out using a spin-coater (Midas system, Spin-1200D). The solutions of oppositely charged GOs were alternately spun coated (30 s at 2000 rpm) onto the substrate with two additional washing steps with DI water between the layer deposition steps. Finally, the LbL-assembled GO thin films were thermally reduced in a furnace with H_2/Ar (1:3) purging at 720 °C. Prepared rGO electrodes were stably stored with dried condition in the desicator for several weeks before use.

2.2. Preparation of LacI-BPA recombinant protein

2.2.1. Construction of plasmid for expression of LacI-BPA

A cysteine-flanked heptapeptide (CKSLENSYC) showing selective affinity to BPA was reported in our previous study (Yang et al., 2014). In the present study, the BPA affinity peptide sequence was inserted at the C-terminus of LacI to create LacI-BPA recombinant protein as shown in Scheme 1 where the peptide moiety possessing affinity to BPA is colored in brick red. The sequence of the fused BPA affinity peptide was inverted to mimic its display at the end of pIII protein on the phage surface. The recombinant plasmid encoding the LacI-BPA was constructed through site-directed mutagenesis using plasmid pWB1000 harboring LacI gene (Kumar et al., 1999) and Muta-Direct™ Site Directed Mutagenesis Kit

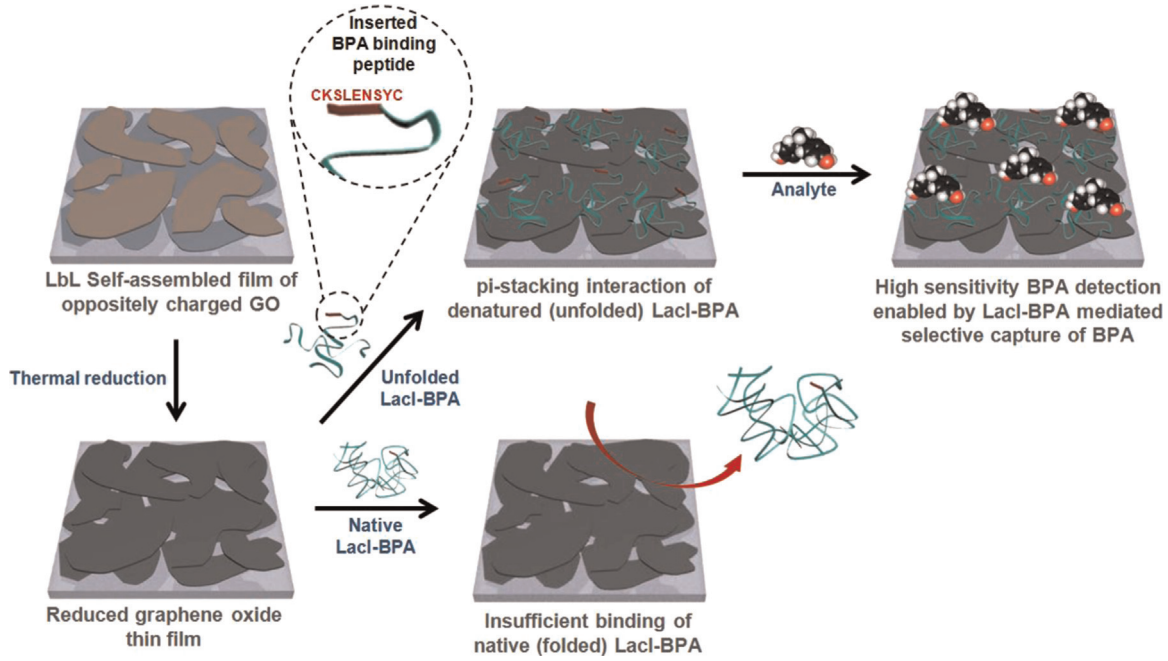

Scheme 1. Schematics of fabricating a BPA sensing platform based on pi-stacking interaction between LacI-BPA recombinant protein and the rGO surface.

(15071, iNtRON biotechnology, Korea). The mutagenic oligonucleotides used were BPA_F (5'-CGGGTGCTACAGCAACGAG CTATCAAAATGCCAG-3') and BPA_R (5'-CTGGCATTTTGATAGCTCG TTGCTGTA GCACCCG-3') where the underlined were DNA sequences encoding the heptapeptide. The correct insertion of the corresponding DNA bases encoding the peptide was confirmed by sequencing the recombinant plasmid.

2.2.2. Expression and purification of LacI-BPA

LacI-BPA was purified according to the protocol described elsewhere (Kumar et al., 1999) with some modifications. Constructed plasmids were transformed into *E. coli* BL21 (DE3) cells for over-expression of LacI-BPA recombinant protein. The transformed cells were grown at 37 °C in dYT media (10 g/L tryptone, 15 g/L yeast extract, 10 g/L NaCl, pH 7.0) containing 50 μg/ml ampicillin for 16 h. After fermentation, cells were harvested and disrupted using a mechanical disruptor operated at 35 kpsi (Constant cell disruption systems, Constant systems Ltd, UK) in Cell Suspension Buffer (CSB) at pH 7.2 (0.2 M Tris–HCl, 0.2 M KCl, 10 mM $MgCl_2$, 5% (v/v) glycerol, 1 mM NaN_3, 0.3 mM DTT and 1 mM PMSF). Cell debris was removed by centrifugation and the supernatant was subsequently subjected to 20–35% ammonium sulfate precipitation. The precipitate at 35% ammonium sulfate was resuspended in 0.05 M KPG buffer at pH 7.2 (0.05 M K_2HPO_4, 1 mM EDTA, 5% (w/v) glucose, 0.03 mM DTT and 1 mM NaN_3) and dialyzed against the same buffer overnight. The dialyzed sample was centrifuged to remove any undissolved materials and the supernatant was loaded into an FPLC (ÄKTAprime™ PLUS, GE Healthcare Life Sciences, Sweden) column packed with cellulose phosphate (P-11, Whatman Int. Ltd, UK). LacI-BPA was eluted with a gradient of 0.05–0.3 M KPG buffer at pH 7.2. The eluted fractions were analyzed by 12% SDS-PAGE, and the concentrations of purified proteins were measured using Quick start Bradford Dye reagent (500-0205, Bio-Rad, USA).

2.3. Fabrication of biosensor and analysis of the sensor performance

An overall procedure for the recombinant protein binding on the surface of rGO thin film is presented in Scheme 1. LacI-BPA solution prepared in water at 0.1 μg/ml was drop-dispensed on the surface of rGO thin film and left in an oven at 70 °C for 30 min. During this incubation period, LacI-BPA recombinant protein was denatured and its immobilization on the rGO thin film was achieved via pi-stacking interaction. After washing with DI water, the rGO thin film electrode layered with denatured LacI-BPA (LacI-BPA/rGO) was used as an impedimetric biosensor for monitoring BPA. As BPA has a low solubility in DI water, it was first dissolved in EtOH at a concentration of 1 μM and subsequently diluted with DI water to give predetermined concentrations of BPA from 100 fM to 10 nM. For BPA detection, 1 ml of BPA solutions at varying concentrations were applied on the LacI-BPA/rGO electrodes and reacted under ambient condition for 30 min. For comparison, BPA analogs (i.e. BPS and BPF solutions prepared at 10 nM) and/or mock samples (i.e. plastic extracts containing BPA and undefined potential interfering species) were tested against the LacI-BPA/rGO electrode in the same manner to record the EIS signals. Mock samples containing BPA with other contaminants were prepared by extracting BPA from arbitrarily collected plastic samples (CD, PC film and PVC glove) according to the reported protocols (Gao et al., 2012; Yu et al., 2011) with minor modification. The plastic products were cut into pieces and cleaned several times with ethanol and DI water. Subsequently, 1.0 g of each sample was added into 50 ml of DI water and heated at 70 °C for 48 h with sealing. After cooling down to room temperature, the solutions were filtered and used as mock samples.

2.4. Measurements and characterizations

Surface topology of the bare and the protein-bound rGO electrodes was investigated using an AFM (Dimension 3100, Veeco, Plainview, NY) in tapping mode under dry condition. Chemical characteristics of the rGO thin films before and after LacI-BPA protein layer deposition were analyzed with a Raman spectrometer system (SENTERRA Raman Microscope, Bruker, MA). EIS was carried out with ZAHNER ENNIUM Electrochemical Workstation in 0.1 M KCl electrolyte with a conventional three-electrode system comprising rGO thin film as a working electrode, platinum wire as a counter electrode and Ag/AgCl as a reference electrode. The impedance spectra were measured in the frequency range of 0.5–10^6 Hz. The amplitude of the applied sine wave potential in

each case was 10 mV. The obtained raw data from EIS measurements were fitted as to the shape of semi-circle drawn from three points of the obtained data and analyzed with the software of CHI Electrochemical Analyzer (CH Instruments, Inc.).

3. Result and discussion

3.1. Preparation of rGO thin film electrode and recombinant LacI-BPA protein

In our previous study, we confirmed a successful functionalization of rGO surface with chemically or thermally denatured BSA proteins (Kim et al., 2013). On the basis of versatility of protein decoration through denaturation, we investigated the adaptability of recombinant proteins on the rGO electrode for realizing a BPA biosensor. A rGO thin film as a working electrode was prepared by spin-assisted LbL self-assembly using oppositely charged GO solutions. An electrostatic interactions between (+) and (−) charged GO nanosheets rendered stacking of GO nanosheets into a multilayer structure. Subsequent thermal treatment turned GO layers into an rGO thin film while removing other functional groups. As shown in Fig. 1A, the rGO thin film comprising 2 bilayers of GOs shows an inter-sheet-connected structure with 3–4 nm in thickness and 0.97 nm in root-mean-square (RMS) roughness, providing the flat and well-covered rGO electrode surface available for further attachment of biomolecules with desired functional property. The "inter-sheet effect" induced from the multilayered stacked structure of rGO nanosheets enables the electrode to precisely detect the binding event of biomolecules occurring on the electrode surface (Rao et al., 2012). Although more tightly packed and thickly stacked films can be fabricated simply by increasing the number of LbL assembly, the expected corresponding increment in surface roughness will undesirably lead to an increase in non-specific binding and/or a substantial loss in sensitivity and selectivity.

A cysteine-flanked heptapeptide (CKSLENSYC) exhibiting high affinity toward BPA was screened by phage display technique and its binding specificity to BPA was confirmed by phage binding assay (Yang et al., 2014). In principle, the heptapeptide moiety cognizant of BPA can be utilized as a sensor probe on rGO electrode for detecting BPA molecules. However, it is difficult to induce direct adhesion of small peptide molecules to chemically neutral rGO surface via pi-stacking interaction unless the peptide is highly enriched with hydrophobic amino acid residues. In order to facilitate direct and stable conjugation of the short length probe peptide with the rGO surface of hydrophobic nature, the aforementioned BPA affinity peptide was docked with LacI protein in such a way that strong hydrophobic interaction with rGO surface could take place upon denaturation of the recombinant protein (LacI-BPA). The LacI used as a docking station was shown to accommodate 9-mer peptide (i.e. SiO_2 and TiO_2 binding peptide 1 (STB1)) without compromising its intrinsic property and/or the solvent accessibility of the fused peptide when the peptide insertion took place between the last two amino acid residues (i.e. glycine and glutamine) located at its C-terminal extreme (Chen et al., 2009). As a result, the purpose-built LacI-BPA used in the present study entails bifunctionality conducive to constructing a rGO based BPA biosensor, in view of providing a protein scaffold prone to denaturation (hence serving for the pi-stacking interaction mediator) and presenting a BPA specific peptide in the context of recombinant protein (hence serving for the BPA selective capture probe).

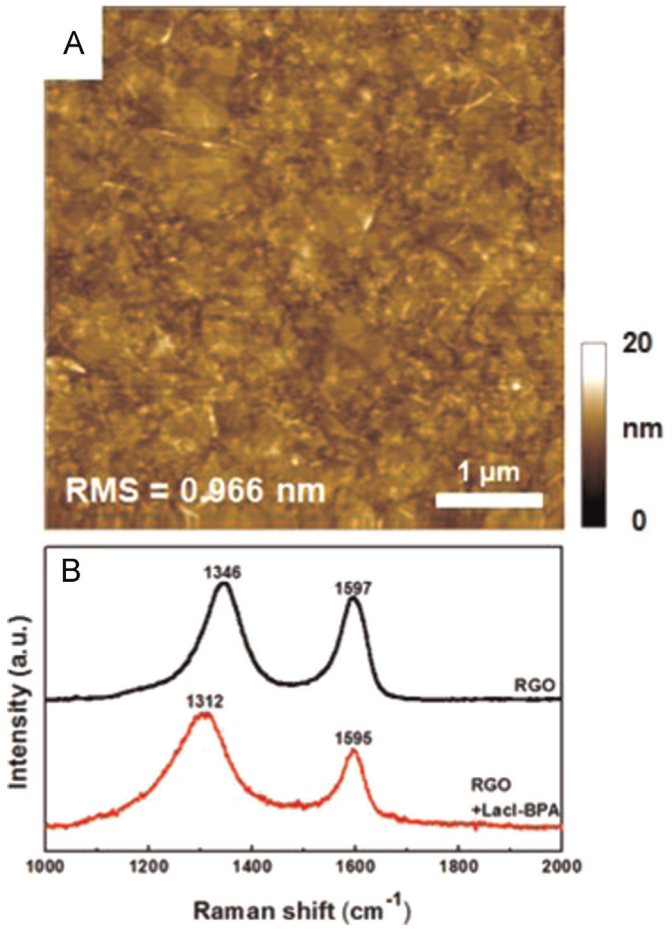

Fig. 1. (A) Two-dimensional AFM image of spin-assisted LBL assembled rGO thin film (scan size=5 × 5 μm^2). (B) Raman spectra of the bare (black) and the denatured LacI-BPA bound (red) rGO thin films. (For interpretation of the references to color in this figure legend, the reader is referred to the web version of this article.)

3.2. Fabrication and characterization of LacI-BPA/rGO biosensor

In general, a majority of proteins in their native forms exhibit unique three dimensional structures whose surfaces are populated, to varying extents, with hydrophilic amino acid residues. While the native status of protein molecules promotes their efficient hydration by water molecules, and hence is conducive to their thermodynamic stability in solution environment, it makes protein molecules hardly compatible with hydrophobic surfaces. In our previous studies where BSA was studied against rGO (Kim et al., 2013) and CVD-grown graphene (Jang et al., 2015), it was found that BSA molecules in denatured form could directly anneal with the graphene surfaces, without any pretreatment, to give rise to highly uniform protein passivated graphene surfaces. This was attributed to the abundant availability of hydrophobic amino acid residues outwardly relocated to the protein exterior upon its unfolding to actively participate in pi-stacking interaction with the graphene surfaces. Since denaturation of protein is critical for their direct adhesion to graphene surface, we decided to fabricate LacI-BPA/rGO sensor with the use of denatured LacI-BPA. Out of the two most common protein denaturation methods (i.e. chemical and heat treatment), the heat denaturation was preferred in our approach in order to obviate any adverse effects that chaotropes and/or reducing agents often present in chemical treatments may exert on the pi-stacking interaction between denatured LacI-BPA and rGO surface. Besides, heat treatment proved more efficient than chemical treatment for completely passivating rGO surface to give

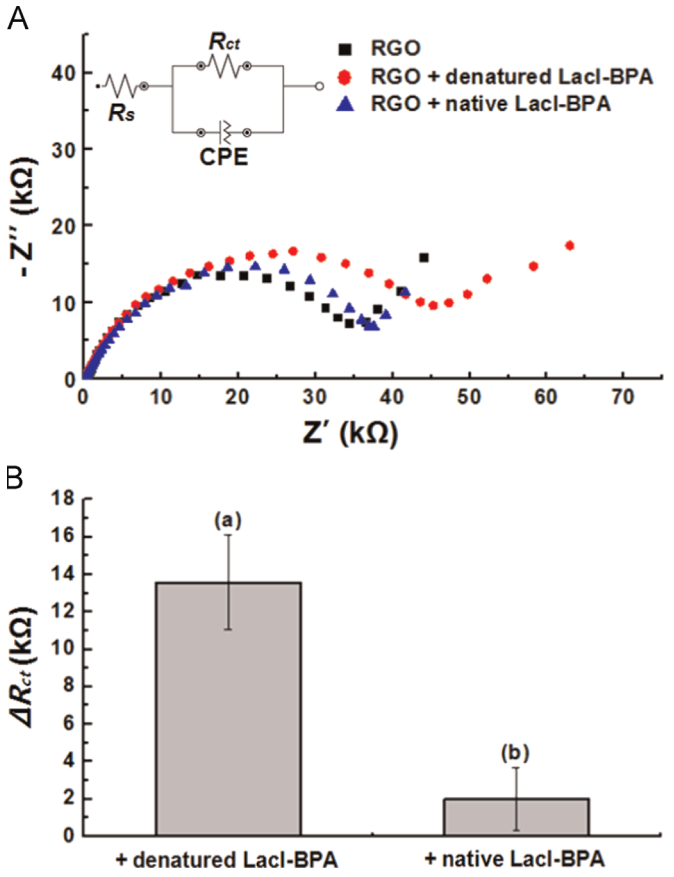

Fig. 2. (A) Nyquist plots and (B) R_{ct} values obtained from bare rGO thin film before and after annealing with native or denatured LacI-BPA recombinant proteins. The inset in panel A shows the equivalent circuit used to model EIS data in the conventional three-electrode system without redox probes where R_{ct}, CPE and R_s represent charge transfer resistance, constant phase element and electrolyte solution resistance, respectively.

more uniform and smooth protein layers (Kim et al., 2013). In order to immobilize LacI-BPA on the rGO electrode surface, 0.1 μg/ml of LacI-BPA solution was dropped on the electrode and left under elevated temperatures (70, 80 and 90 °C) for varying incubation periods (10, 20 and 30 min). Since the adsorption of the LacI-BPA protein on rGO surface is nonspecific and the whole rGO surface is hard to be uniformly covered with LacI-BPA molecules due to their propensity for aggregation upon denaturation. We therefore focused our attention on designing of the LacI-BPA/rGO electrode passivated fully with denatured LacI-BPA in order to obviate the necessity of any backfill process and/or to avoid any noise signals possibly arising from background binding of many undefined species contained in the actual samples. By carefully controlling the protein adsorption conditions on the rGO electrode in view of protein concentration, incubation temperature and time, we found the optimized condition for attaining the fully covered rGO surface with non-clustered proteins of the denatured LacI-BPA probe (this will be shown in Fig. 3). It was noted that with the presence of rGO electrode during heat denaturation of LacI-BPA, pi-stacking interaction between denatured protein and rGO surface was preferred, rather than formation of insoluble protein coagulates due to self-aggregation among denatured protein molecules. However, it was found that the denatured LacI-BPA molecules were prone to self-aggregation when the incubation temperature was higher than 70 °C. In addition, the incubation time of 30 min was essential for complete denaturation of LacI-BPA. Hence, among the conditions tested, 30 min incubation at 70 °C was found to be optimum in terms of achieving uniformly layered LacI-BPA on rGO electrode with an almost complete surface coverage.

Importantly, our BPA sensing platform LacI-BPA/rGO fabricated as above does not require any backfill process (due to the complete surface coverage) or interlayer insertion process between the probe and the electrode (due to the direct pi-stacking adhesion). Raman spectroscopy was employed to confirm the successful binding of recombinant LacI-BPA on rGO electrode. As shown in Fig. 1B, pristine rGO film shows typical peak responses at 1346 and 1597 cm^{-1}, corresponding to the well documented D and G bands of graphene, respectively (Ni et al., 2008). On the other hand, upon attachment of denatured LacI-BPA, Raman spectra peaks for LacI-BPA/rGO become broader and blue-shifted to 1312 and 1595 cm^{-1} for D and G bands. This implies that the denatured proteins interact with hydrophobic rGO surface through pi-stacking interaction (Li et al., 2012), eventually leading to an efficient formation of

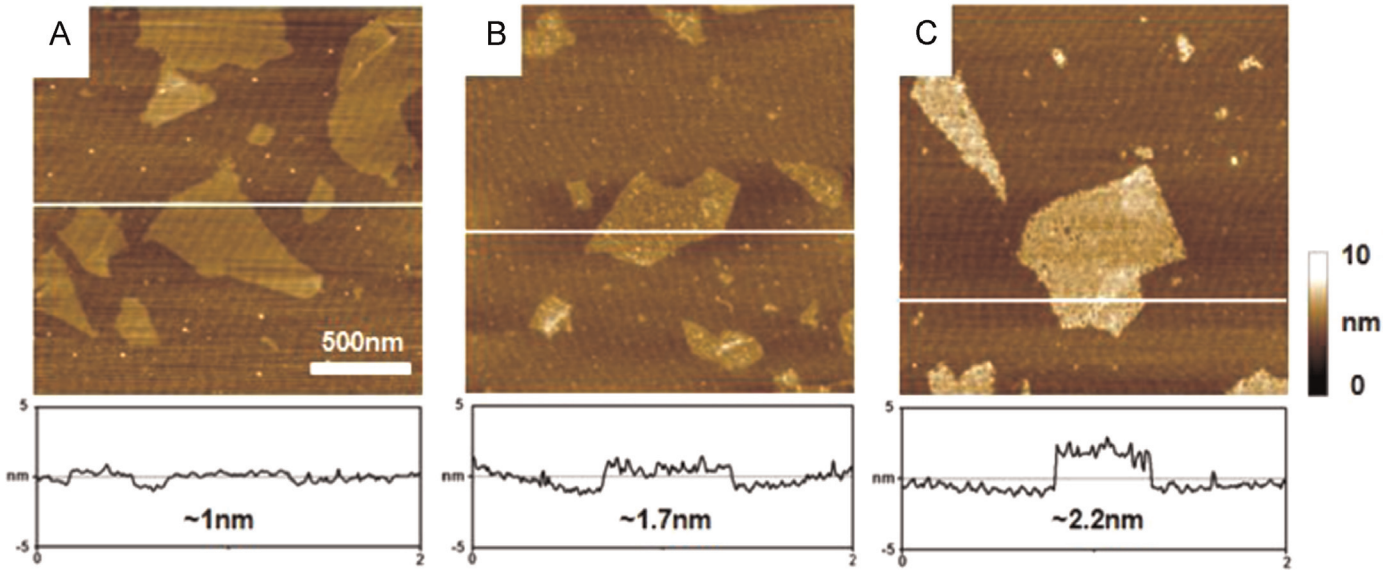

Fig. 3. Two-dimensional (top) and cross-sectional (bottom) AFM images to show stepwise changes in the rGO surfaces according to adsorption of probe and/or target molecules (scan size = 2 × 2 $μm^2$). White lines indicate the sectioned regions. (A) Bare rGO surface. (B) Direct adhesion of denatured LacI-BPA with rGO (LacI-BPA/rGO). (C) BPA binding on rGO layered with denatured LacI-BPA (BPA/LacI-BPA/rGO).

rGO electrode layered with denatured LacI-BPA.

EIS was used to monitor the changes in electrochemical characteristics of the rGO electrodes. Fig. 2A shows Nyquist plots for rGO electrodes before and after the attachment of native or denatured LacI-BPA recombinant proteins. In the Nyquist plot, the diameter of semi-circle observed in high frequency domain corresponds to a charge transfer resistance (R_{ct}), indicating the extent of interfacial resistance experienced for the charge transfer process at the electrode surface before and after protein adsorption. The changes in R_{ct} values (ΔR_{ct}) upon binding of denatured and native LacI-BPA on the pristine rGO thin films are presented in Fig. 2B. The R_{ct} value of bare rGO electrode was measured to be 39.7 kΩ. After binding of denatured LacI-BPA, the value increased to 53.3 kΩ to give ΔR_{ct} of 13.6 kΩ. This is presumed to occur due to efficient adhesion of a large amount of denatured LacI-BPA molecules on the rGO surface, which insulates the electrode and hampers the access of the electrolytes to the electrode surface. In contrast, passivation of the rGO electrode with native LacI-BPA resulted in a small increase in R_{ct} (i.e. ΔR_{ct}=2.0 kΩ), significantly lower compared with the denatured LacI-BPA case. This confirms further the necessity of the heat denaturation process for inducing successful pi-stacking mediated binding interaction between recombinant LacI-BPA and rGO surfaces. The R_{ct} measurement using EIS also offers a useful clue to determine the protein concentration to give a uniform coverage of the rGO electrode with densely spread protein layer. The use of excessive amount of protein at the time of rGO electrode passivation gives rise to rugged protein islands randomly scattered on the rGO surface due to self-aggregation of denatured protein molecules, largely resulting in irregular ΔR_{ct} fluctuating in a broad range, which makes it difficult to obtain reproducible sensor performances.

3.3. Sensing performance for BPA detection

One concern associated with the use of denatured proteins as a sensor probe is that they may fail to specifically recognize their target analytes due to denaturation-triggered inadvertent changes in 3D and/or local structures often presumed to affect the accessibility to their binding partners. In our previous study, heat-denatured BSA was demonstrated to retain its specific binding affinity to anti-BSA antibody (Kim et al., 2013), since the epitope residing in BSA recognized anti-BSA antibody regardless of whether BSA being in native or denatured form (Kolusheva et al., 2001). However, it is cautious to generalize this particular example to the LacI-BPA interaction with BPA. In order to address this issue, we attempted to clearly visualize the adsorption of denatured LacI-BPA and the according interaction with BPA on the surface of rGO electrode by atomic force microscopic (AFM), for which the rGO-covered electrode samples were prepared with reduced concentration of GO solution (1/20 of the original solution concentration).

As shown in Fig. 3A, exfoliated rGO nanosheets with a thickness of ~1 nm are sparsely distributed and clearly discerned from the background substrate. After binding of the denatured LacI-BPA, the entire film thickness increased to 1.7 nm. In contrast, for the control experiment conducted with native LacI-BPA, no significant change in the surface topology was observed. The specific binding capability of the denatured LacI-BPA with BPA molecules is manifested in Fig. 3C, where the cross-sectional film thickness further increased to 2.2 nm. This implies that the insertion of BPA affinity heptapeptide moiety to the extreme C-terminus of LacI does not affect its solvent accessibility to BPA, and that thermal denaturation would least affect the affinity of the recombinant LacI-BPA to BPA molecules.

LacI-BPA bound rGO electrodes were tested for quantitative detection of BPA. Fig. 4A clearly shows that R_{ct} gradually increases with increasing BPA concentration. Plotting the R_{ct} values with respect to the logarithmic BPA concentrations exhibits a linear dynamic response range from 100 fM to 10 nM as shown in Fig. 4B. A detection limit of the proposed sensing platform was calculated to be 5.0 fM from the calibration curve (Thompson and Ellison, 2002). When BPA concentration exceeds 10 nM, however, the R_{ct} increment (ΔR_{ct}) drastically increases and results in non-linearity, which is possibly associated with the multilayer adsorption of BPA on the electrode surface. As control experiments, 10 nM of BPA was applied to a bare and/or denatured wild type LacI coated rGO electrodes. As shown in Fig. 4A (inset), no significant changes in EIS were found from these electrodes, indicating that BPA rarely interacts with the bare rGO surface itself or with the wild type LacI lacking BPA affinity peptide moiety. According to the report from the United States Environmental Protection Agency (USEPA) and related studies, acceptable daily intake (ADI) of BPA is 50 μg/kg-body weight (Vom Saal and Welshons, 2006), which is equivalent to 30–35 μg/kg-water (or approximately 220–257 nM) considering

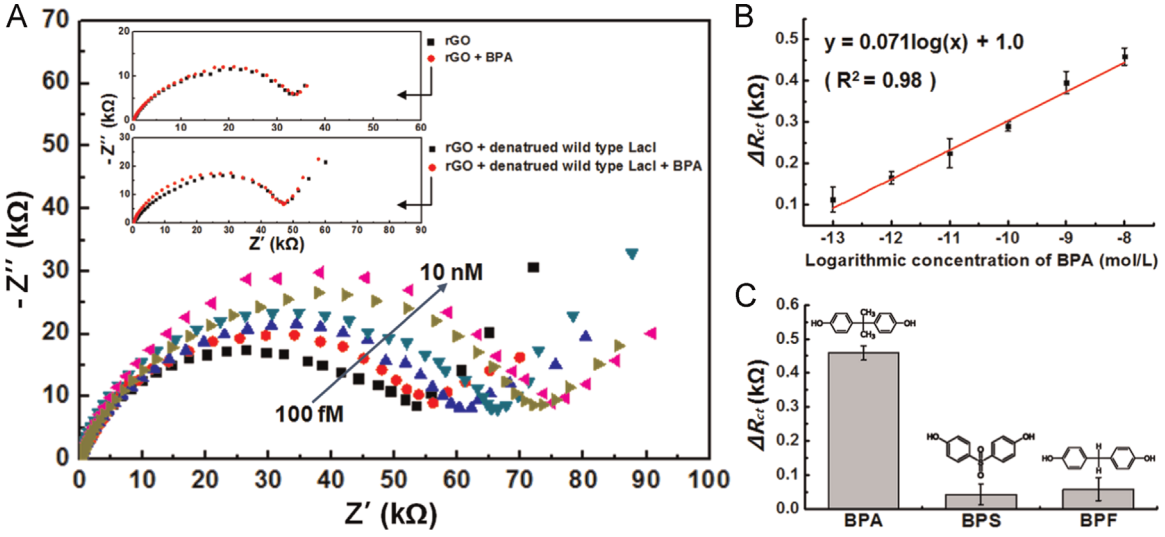

Fig. 4. (A) Nyquist plots of the LacI-BPA/rGO electrode based biosensor for BPA detection from 100 fM to 10 nM. The inset shows the negligible EIS responses for control cases where 10 nM of BPA was applied to bare (top) and wild type LacI layered (bottom) rGO electrodes. (B) Plot of increment in R_{ct} vs logarithmic concentrations of BPA. (C) Assessment of selectivity of the BPA sensor against 10 nM of BPA analogs such as BPS and BPF.

Table 1
Assessment of spike recovery efficiency of the LacI-BPA/rGO sensor from the plastic extracts containing BPA and other undefined contaminants.

Sample	BPA concentration			RSD[b]	Recovery[c]
	Before spiking (pM)	Spiked (pM)	After spiking[a] (pM)	(%)	(%)
CD	1.89	10	12.48	2.7	106
PC film	6.30	10	15.65	4.5	94
PVC glove	157.95	500	631.81	7.1	95

[a] Mean value of three individual measurements.
[b] RSD: relative standard deviation for three individual measurements.
[c] Recovery=(BPA after spiking – BPA before spiking)/(BPA spiked) × 100.

that 60–70% of body is made up of water. In addition, FDA's Center for Food Safety and Applied Nutrition (CFSAN) presented that an average dietary exposure to BPA is 0.2–0.4 μg/kg-body weight (0.12–0.28 μg/kg-water, 0.5–1.2 nM) for infants. The sensor system presented in this study is well suited for practical determination of BPA in a wide concentration range inclusive of its dietary exposure level and ADI.

3.4. Selectivity analysis

Finally, the detection selectivity of BPA sensors was investigated with the use of BPA analogs; BPS and BPF having similar structures with BPA were chosen to confirm the specific affinity of LacI-BPA probe toward BPA molecules. Following the same procedure as described above, 10 nM of BPS or BPF solution was incubated with LacI-BPA/rGO electrode for 30 min at room temperature and the corresponding ΔR_{ct} was measured and compared with that from BPA. As shown in Fig. 4C, upon applying BPS and BPF, the R_{ct} increments were observed to be 0.042 and 0.058, respectively. These changes are negligible as compared with the ΔR_{ct} of 0.46 recorded from BPA at the same concentration, which indicates that the LacI-BPA/rGO sensor developed in this study is highly specific for BPA.

3.5. Spike recovery test

Spike recovery experiments were further conducted to assess any interfering effects on accurate detection of BPA that might be exerted by various undefined species co-present with BPA. In order to mimic this complicated actual sensing environment, the mock samples (i.e. plastic extracts containing BPA and other contaminants) were prepared as described in Section 2.3. The extents of possible interference with BPA detection in actual samples were assessed by spiking predetermined amounts of BPA into the mock samples and subsequently calculating BPA concentrations from the changes in ΔR_{ct} values before and after the spiking. As summarized in Table 1, our LacI-BPA/rGO sensor shows excellent recoveries of spiked BPA (94–106%) from three different mock samples tested, each with relative standard deviation of less than 7.1% for three independent measurements. This indicates its practical applicability to actual samples containing BPA and many other undefined contaminants.

4. Conclusion

In this study, graphene-based impedance biosensor for BPA detection was fabricated by direct annealing of recombinant protein probe selectively recognizing BPA (LacI-BPA) with rGO thin film electrode. The recombinant LacI-BPA arising from insertion of cysteine-flanked high affinity BPA binding peptide (CKSLENSYC) at the C-terminal extreme of LacI protein showed its superb self-adhesion in denatured form to the rGO electrode surface while preserving its solvent accessibility and affinity to BPA after the adsorption. The uniform and complete passivation of rGO surface with denatured LacI-BPA also provided abundant probe molecules readily available on the electrode surface to capture BPA, while obviating the blocking procedure often required elsewhere to minimize background noise signals. As a result, the use of denatured LacI-BPA led to facile construction of a highly sensitive LacI-BPA/rGO impedimetric BPA sensor able to detect BPA in a broad linear dynamic detection range from 100 fM to 10 nM. Furthermore, our LacI-BPA/rGO sensor showed minimal cross reactivity toward BPA analogs, and almost complete recoveries of spiked BPA in the presence of various potential interfering species extracted from plastic products. These merits will render the developed BPA sensor suitable for practical applications where sensitive and selective BPA determination is of critical concern. In addition, the method demonstrated for interfacing protein with hydrophobic rGO surface would provide a novel platform strategy for generation of various sensing platforms where direct compatibility between the probe molecules and the sensor surfaces matters.

Acknowledgments

This work was supported by research grants of NRF, South Korea (2012M1A2A2671795, 2014M3A7B4052200, and 2014M3C1A3053035) and Basic Science Research Program (2010-0027955) funded by the National Research Foundation under the Ministry of Science, ICT and Future Planning, Korea.

References

Altamirano, J.C., Fontana, A.R., de Toro, M.M., 2011. J. Agric. Food Chem. 59, 3559–3565.
Cao, G.S., Wang, R.L., Wang, P.L., Li, X., Wang, Y., Wang, G.L., Li, J.P., 2014. Nano 9, 1450047. http://dx.doi.org/10.1142/S1793292014500477.
Castro Neto, A.H., Guinea, F., Peres, N.M.R., Novoselov, K.S., Geim, A.K., 2009. Rev. Mod. Phys. 81, 109–162.
Chen, H., Su, X., Neoh, K.G., Choe, W.S., 2009. Adv. Funct. Mater. 19, 1186–1192.
Gao, Y., Cao, Y., Yang, D., Luo, X., Tang, Y., Li, H., 2012. J. Hazard. Mater 199-200, 111–118.
Geim, A.K., Novoselov, K.S., 2007. Nat. Mater. 6, 183–191.
Hummers, W.S., Offeman, R.E., 1958. J. Am. Chem. Soc. 80 1339–1339.
Jang, S.K., Jang, J.R., Choe, W.S., Lee, S.J., 2015. ACS Appl. Mater. Interfaces 7, 1250–1256.
Kafi, M.A., Kim, T.H., An, J.H., Choi, J.W., 2011. Biosens. Bioelectron. 26, 3371–3375.
Kim, K.S., Um, Y.M., Jang, J.R., Choe, W.S., Yoo, P.J., 2013. ACS Appl. Mater. Interfaces 5, 3591–3598.
Kolusheva, S., Kafri, R., Katz, M., Jelinek, R., 2001. J. Am. Chem. Soc. 123, 417–422.
Kubesa, O., Morrisey, K., Mathews, S., Proetta, J., Li, C., Skladal, P., Hepel., M., 2014. Mediterr. J. Chem. 3, 916–928.
Kuiper, G.G.J.M., Lemmen, J.G., Carlsson, B., Corton, J.C., Safe, S.H., van der Saag, P.T., van der Burg, B., Gustafsson, J.A., 1998. Endocrinology 139, 4252–4263.
Kumar, A., Galaev, I.Y., Mattiasson, B., 1999. Bioseparation 8, 307–316.
Kuroda, N., Kinoshita, Y., Sun, Y., Wada, M., Kishikawa, N., Nakashima, K., Makino, T., Nakazawa, H., 2003. J. Pharm. Biomed. Anal. 30, 1743–1749.
Li, H.Q., Han, L.N., Cooper-White, J.J., Kim, I., 2012. Nanoscale 4, 1355–1361.
Lin, C.Y., Fuh, M.R., Huang, S.D., 2011. J. Sep. Sci. 34, 428–435.
Long, F., Zhu, A., Zhou, X., Wang, H., Zhao, Z., Liu, L., Shi, H., 2014. Biosens. Bioelectron. 55, 19–25.
Macdonald, J.R., 1987. Impedance Spectroscopy. Wiley, New York.
Mei, Z., Chu, H., Chen, W., Xue, F., Liu, J., Xu, H., Zhang, R., Zheng, L., 2013b. Biosens. Bioelectron. 39, 26–30.
Mei, Z., Qu, W., Deng, Y., Chu, H., Cao, J., Xue, F., Zheng, L., El-Nezamic, H.S., Wu, Y., Chen, W., 2013a. Biosens. Bioelectron. 49, 457–461.
Ni, Z.H., Wang, Y.Y., Yu, T., Shen, Z.X., 2008. Nano Res. 1, 273–291.
Park, J.S., Cho, S.M., Kim, W.J., Park, J., Yoo, P.J., 2011. ACS Appl. Mater. Interfaces 3, 360–368.
Rao, F.B., Almumen, H., Fan, Z., Li, W., Dong, L.X., 2012. Nanotechnology 23, 105501.

Rodriguez-Mozaz, S., de Alda, M.L., Barcelo, D., 2005. Water Res. 39, 5071–5079.
Staples, C.A., Dorn, P.B., Klecka, G.M., O' Block, S.T., Harris, L.R., 1998. Chemosphere 36, 2149–2173.
Stobiecka, M., Chałupa, A., 2015. Chem. Pap. 69, 62–76.
Stobiecka, M., Hepel, M., 2011. Biosens. Bioelectron. 26, 3524–3530.
Stobiecka, M., Molinero, A.A., Chałupa, A., Hepel, M., 2012. Anal. Chem. 84, 4970–4978.
Thompson, M., Ellison, S.L.R., Wood, R., 2002. Pure Appl. Chem. 74, 835–855.
Vandenberg, L.N., Hauser, R., Marcus, M., Olea, N., Welshons, W.V., 2007. Reprod. Toxicol. 24, 139–177.
Vom Saal, F.S., Hughes, C., 2005. Environ. Health Perspect. 113, 926–933.
Vom Saal, F.S., Welshons, W.V., 2006. Environ. Res. 100, 50–76.
Wang, K., Ruan, J., Song, H., Zhang, J.L., Wo, Y., Guo, S.W., Cui, D.X., 2010. Nanoscale Res. Lett. 6, 8.
Wang, X., Reisberg, S., Serradji, N., Anquetin, G., Pham, M.C., Wu, W., Dong, C.Z., Piro, B., 2014. Biosens. Bioelectron. 53, 214–219.
Wang, X., Zeng, H.L., Zhao, L.X., Lin, J.M., 2006. Anal. Chim. Acta 556, 313–318.
Wu, L., Deng, D., Jin, J., Lu, X., Chen, J., 2012. Biosens. Bioelectron. 35, 193–199.
Yang, J., Kim, S.E., Cho, M., Yoo, I.K., Choe, W.S., Lee, Y., 2014. Biosens. Bioelectron. 61, 38–44.
Yu, C., Gou, L., Zhou, X., Bao, N., Gu, H., 2011. Electrochim. Acta 56, 9056–9063.
Zhu, L., Cao, Y., Cao, G., 2014. Biosens. Bioelectron. 54, 258–261.